



where  $k_d$  is the phase-to-voltage gain, the symbol “ $\leftrightarrow$ ” stands for the Fourier transform inverse-transform pair, and time and frequency ( $t$  and  $f$ ) are implied. The single-sided cross PSD is

$$S_{\eta\xi} = \frac{2}{\mathcal{T}} \mathcal{Y} \mathcal{X}^* \quad (\text{cross PSD}) \quad (5)$$

where the factor ‘2’ accounts for the power at negative frequencies,  $\mathcal{T}$  is the acquisition time for each realization (we may let  $\mathcal{T} \rightarrow \infty$  in theoretical issues), and the superscript ‘\*’ means complex conjugate. After averaging out the single-channel noise, the cross spectrum is

$$S_{\eta\xi} = k_d^2 \frac{2}{\mathcal{T}} |\Phi|^2 = k_d^2 S_\varphi \quad (6)$$

The equation generally used for the instrument readout is

$$S_\varphi = \frac{1}{k_d^2} S_{\eta\xi} \quad (\text{readout}). \quad (7)$$

### B. Spectral Estimation

However simple, the proof of (6) provides insight. We introduce the notation  $\mathbb{E}\{\}$  for the mathematical expectation;  $\langle \rangle_m$  for the average on  $m$  realizations; the ‘hat’ accent, as in  $\hat{S}$ , for the estimator; and the superscript ‘prime’ and ‘second’ for the real and imaginary part of a variable, as in  $\Phi = \Phi' + i\Phi''$ . Expanding (5) we find

$$\Re\{S_{\eta\xi}\} = \frac{2}{\mathcal{T}} \left\{ k_d^2 (\Phi'^2 + \Phi''^2) + k_d [\Phi' (\mathcal{N}'_1 + \mathcal{N}'_2) + \Phi'' (\mathcal{N}''_1 + \mathcal{N}''_2)] + \mathcal{N}'_1 \mathcal{N}'_2 + \mathcal{N}''_1 \mathcal{N}''_2 \right\} \quad (8)$$

$$\Im\{S_{\eta\xi}\} = \frac{2}{\mathcal{T}} \left\{ k_d [\Phi' (-\mathcal{N}''_1 + \mathcal{N}''_2) + \Phi'' (\mathcal{N}'_1 - \mathcal{N}'_2)] + \mathcal{N}'_1 \mathcal{N}''_2 - \mathcal{N}''_1 \mathcal{N}'_2 \right\}. \quad (9)$$

Still not accounting for thermal energy in the power splitter, we can assume that  $\Phi$ ,  $\mathcal{N}'_1$  and  $\mathcal{N}'_2$  are statistically independent. Taking the expectation of (8) and (9), we get

$$\mathbb{E}\{S_{\eta\xi}\} = k_d^2 \frac{2}{\mathcal{T}} \mathbb{E}\{|\Phi|^2\} + i0 \quad (\text{expectation}). \quad (10)$$

The term ‘ $i0$ ’ in (10) emphasizes the fact that all the useful signal (the DUT noise) goes in  $\Re\{S_{\eta\xi}\}$ .

Actual measurements rely on an estimator. After (7) and (10)

$$\hat{S}_\varphi = \frac{1}{k_d^2} \langle \Re\{S_{\eta\xi}\} \rangle_m \quad (\text{estimator}) \quad (11)$$

is an obvious choice because this is estimator is unbiased

$$\mathbb{E}\{\hat{S}_{\eta\xi}\} = \mathbb{E}\{\langle \Re\{S_{\eta\xi}\} \rangle_m\} = \mathbb{E}\{S_{\eta\xi}\}$$

### III. THERMAL ENERGY IN THE INPUT POWER SPLITTER

Starting from this Section, we analyze the thermal noise of the input power splitter, and its consequences on the measurement of  $S_\varphi$ . The simplest way to understand the problem is to focus on thermal noise associated to the RF signals  $x$  and  $y$  of Fig. 1 (see also Fig. 2, discussed later). The PSD of the

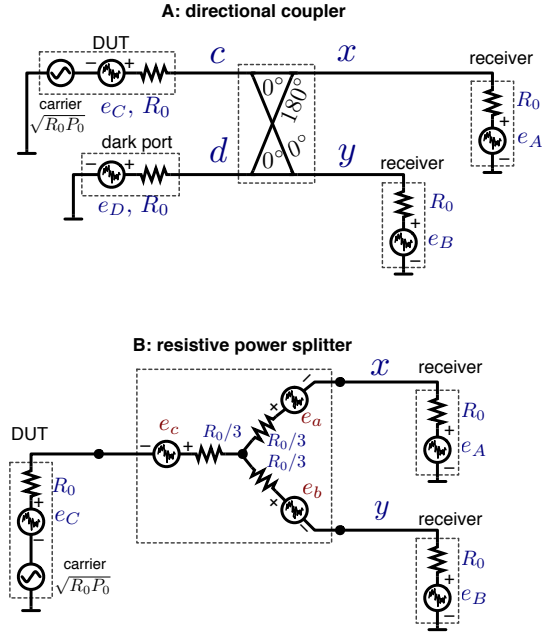


Fig. 2. Power splitters.

available voltage is equal to  $kTR_0$ , where  $k = 1.38 \times 10^{-23}$  is the Boltzmann constant,  $T$  is the equivalent temperature, and  $R_0$  the characteristic impedance. For reference, the thermal emf in 1 Hz bandwidth  $e_n$  across a resistor  $R$  is ruled by  $\mathbb{E}\{e_n^2\} = 4kTR$ , thus  $e_n$  is of 0.9 nV/ $\sqrt{\text{Hz}}$  with  $R = 50 \Omega$  at room temperature.

Following this approach, the phase detector is seen as a *receiver* described in terms of *back radiation* temperature  $T_R^*$ , the same for the two channels. The reason is that the noise radiated back from the output generates crosstalk if the channels are not isolated, and in turn may contribute to the background noise. By contrast, the ‘regular’ noise temperature  $T_R$  give no information of the fraction of noise averaged out or kept through crosstalk. The receiver can be a double balanced mixer as in Fig. 1, or a more complex phase detector, as the interferometer [5], [6].

The problem is therefore to estimate the additive noise  $S_c = kT_C R_0$  of signal  $c$  from  $S_{\eta\xi}$ , and then to estimate  $S_\varphi$  using

$$S_\varphi(f) = \frac{kT_C}{P_0} = \frac{S_c}{R_0 P_0} \quad (12)$$

where  $P_0$  is the carrier power.

#### A. Loss-Free Power Splitter

The 4-port directional coupler terminated at one input (dark port) is by far the preferred power splitter (Fig. 2 A). Dropping the carrier, the coupler output signals are

$$x = \frac{1}{2\sqrt{2}} (e_C - e_D) + \frac{1}{2} e_A$$

$$y = \frac{1}{2\sqrt{2}} (e_C + e_D) + \frac{1}{2} e_B$$

where the terms ‘ $e$ ’ are the resistors’ thermal emfs [V/ $\sqrt{\text{Hz}}$ ], all statistically independent. The equivalent temperature is

$T_C = PS_\varphi/k$  for the oscillator's noise floor, and  $T_D$  for the dark port. Trite calculation gives

$$\begin{aligned}\mathbb{E}\{S_{yx}\} &= \frac{1}{8} \left[ \mathbb{E}\{e_C^2\} - \mathbb{E}\{e_D^2\} \right] \\ &= \frac{1}{2} \mathbb{E}\{S_c\} - \frac{1}{2} \mathbb{E}\{S_d\}\end{aligned}\quad (13)$$

$$= \frac{1}{2} k [T_C - T_D] R_0 \quad (14)$$

Equation (14) is the physical principle of the correlation radiometer [10], and also used in Johnson thermometry [11]. In this case, the instrument measures the temperature  $\Delta T = T_C - T_D$  using the estimator

$$\widehat{\Delta T} = \frac{2}{kR_0} \langle \Re\{S_{yx}\} \rangle_m \quad (\text{thermometer, radiometer}) \quad (15)$$

Back to phase noise, the rigorous evaluation of phase noise results from (12) and (13), which gives the unbiased estimator

$$\begin{aligned}\hat{S}_\varphi &= \frac{2\hat{S}_{yx}}{R_0P_0} + \frac{kT_D}{P_0} \\ &= \frac{2\hat{S}_{\eta\xi}}{k_d^2R_0P_0} + \frac{kT_D}{P_0}\end{aligned}\quad (\text{unbiased estimator}) \quad (16)$$

By contrast, discarding the thermal energy of the dark port results in the biased estimator

$$\hat{S}_\varphi = \frac{2\hat{S}_{yx}}{R_0P_0} = \frac{2\hat{S}_{\eta\xi}}{k_d^2R_0P_0} \quad (\text{biased estimator}) \quad (17)$$

The bias, defined as  $\Delta S_\varphi = \hat{S}_\varphi - \mathbb{E}\{S_\varphi\}$  and given by

$$\Delta S_\varphi = -\frac{kT_D}{P_0} \quad (\text{bias}) \quad (18)$$

results in a systematic *under-estimation* of the DUT noise.

### B. Resistive Power Splitter

The Y resistive power splitter (Fig. 2B) is sometimes used instead of the directional coupler, for example in the Keysight E5500 series [13]. Dropping the carrier, the signals at the splitter output are

$$x = \frac{1}{2}e_A + \frac{1}{4}e_B + \frac{1}{4}e_C - \frac{1}{2}e_a + \frac{1}{4}e_b + \frac{1}{4}e_c \quad (19)$$

$$y = \frac{1}{4}e_A + \frac{1}{2}e_B + \frac{1}{4}e_C + \frac{1}{4}e_a - \frac{1}{2}e_b + \frac{1}{4}e_c \quad (20)$$

The emfs 'e' are all statistically independent, and governed by  $\mathbb{E}\{e^2\} = 4kTR$ , with  $R = R_0$  for the DUT and the receivers,  $R = R_0/3$  for the splitter's internal resistors,  $T = T_C$  for the DUT,  $T = T_R^*$  for the receivers, and  $T = T_S$  for the splitter's internal resistors. The cross PSD at the splitter output is

$$\mathbb{E}\{S_{yx}\} = k \left( \frac{1}{4}T_C - \frac{1}{4}T_S + T_R^* \right) R_0 \quad (21)$$

$$= \frac{1}{4}S_c + k \left( T_R^* - \frac{1}{4}T_S \right) R_0 \quad (22)$$

The unbiased estimator is obtained combining (12) and (22)

$$\begin{aligned}\hat{S}_\varphi &= \frac{4\hat{S}_{yx}}{R_0P_0} + \frac{k(T_S - 4T_R^*)}{P_0} \\ &= \frac{4\hat{S}_{\eta\xi}}{k_d^2R_0P_0} + \frac{k(T_S - 4T_R^*)}{P_0}\end{aligned}\quad (\text{unbias. estimator}) \quad (23)$$

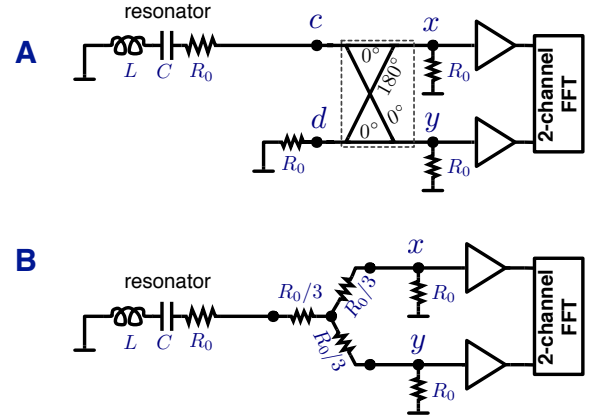


Fig. 3. Experimental configurations.

where  $\hat{S}_{\eta\xi}$  is given by (11). Neglecting the splitter's thermal energy results in the biased estimator

$$\hat{S}_\varphi = \frac{4\hat{S}_{yx}}{R_0P_0} = \frac{4\hat{S}_{\eta\xi}}{k_d^2R_0P_0} \quad (\text{biased estimator}) \quad (24)$$

whose bias is given by

$$\Delta S_\varphi = -\frac{k(T_S - 4T_R^*)}{P_0} \quad (\text{bias}). \quad (25)$$

Unlike the directional coupler, the systematic error can be either positive or negative.

## IV. THE CHALLENGING OSCILLATORS

Lowest white noise at a given physical temperature is achieved by bandpass filtering between the core oscillator and the output buffer, and with a special design of the output buffer. A single resonator is used as the reference resonator and as the output filter. This design solves the issue of harmonic distortion and circumvents the white phase noise of the oscillator [14] (See also [15, p. 264] for the electrical diagram of a complete oscillator). There results a white floor just above the thermal floor.

The key point is that the the current flowing in the quartz is transferred to the output with a minimum noise contribution of the buffer, which is a common-base amplifier. Out of the quartz bandwidth, the motional resistance is not coupled to the buffer, and the white noise of the sustaining amplifier is not transferred to the buffer.

## V. EXPERIMENTS

Given the additive nature of the white PM noise, the presence of a carrier signal is not necessary, and we can work with the RF noise trusting  $b_0 = kT/P$ . Our experiments (Fig 3) are inspired to the internal configuration of the low-noise oscillators, where a resonator is used as the output filter [14].

Having said that, we decided to work on mockup where the frequency is scaled down by a factor of  $10^5$ , i.e., 1 kHz instead of 100 MHz. The reason for this choice is that we have full control on the receiver (regular) noise temperature  $T_R$  and on

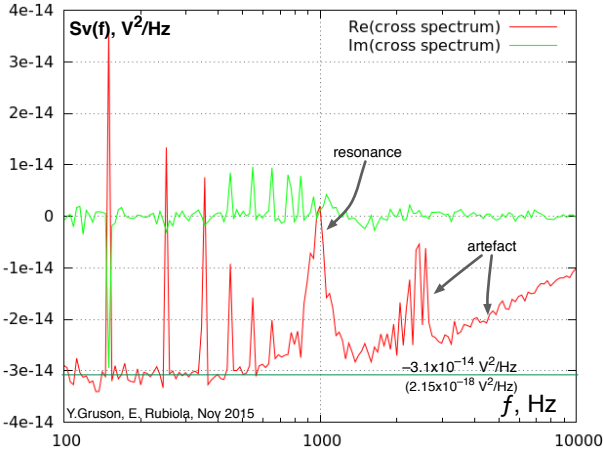


Fig. 4. Cross spectrum measured with the configuration of Fig. 3 A.

the back-scatter temperature  $T_R^*$ . In fact, working with JFET operational amplifiers (AD 743) at low  $R_0$  ( $< 10$  k $\Omega$ ) as the receiver, the input current noise is negligible, and gives rise to no crosstalk even with large-size averaging. Thus it holds that  $T_R^* = T_{ph} \approx 300$  K, the physical temperature of the amplifier. The noise temperature  $T_R$  is of the order of 1500 K, which is rejected by averaging the cross spectrum.

All the experiments are done in a shielded chamber with proportional-integral control of temperature and humidity, and the critical circuits are further shielded in a mumetal enclosure borrowed from an atomic-clock experiment.

#### A. First Experiment

In the first experiment (Fig. 3 A) we use a custom directional coupler based on traditional transformers with laminated silicon steel core. Recycling surplus parts, we ended up with a trivial  $1 : \sqrt{2}$  voltage ratio, hence  $R_0$  is of 300  $\Omega$  on the left-hand side and of 600  $\Omega$  on the right-hand side. The resonator is implemented with a 470 mH olla ferrite inductor and a mylar capacitor, resonating at 1 kHz with  $Q = 5$  (loaded) and  $R_0 = 300$   $\Omega$ .

The spectrum, obtained after a few thousands of FFT acquisitions for convergence, is shown on Fig. 4. At the resonance, the coupler is loaded to two equal resistors  $R_0$  at the same temperature. The cross-spectrum  $S_{yx}$  is equal to zero, as predicted by Eq. (14). Off resonance, the resonator is seen as open circuit ( $\Gamma = 1$ ), for there is no thermal noise to  $x$  and  $y$ . Conversely, the signal  $d$  is anti-correlated at the two outputs, as seen from the phase relationships  $0^\circ$  and  $180^\circ$  on the coupler. The real part  $\Re\{S_{yx}\}$  is of about  $-2.2 \times 10^{-18}$  V<sup>2</sup>/Hz. This is in fairly good agreement with the value of  $-2.5 \times 10^{-18}$  predicted by Eq. (14) with  $R_0 = 600$   $\Omega$  (at the right-hand side of the coupler). Notice that  $\Im\{S_{yx}\}$  is close to zero at all frequencies, as expected.

#### B. Second Experiment

The second experiment (Fig. 3 B) uses a Y power splitter implemented with three  $R_0/3 = 100$   $\Omega$  metal-film resistors, while the resonator is the same as in the first experiment.

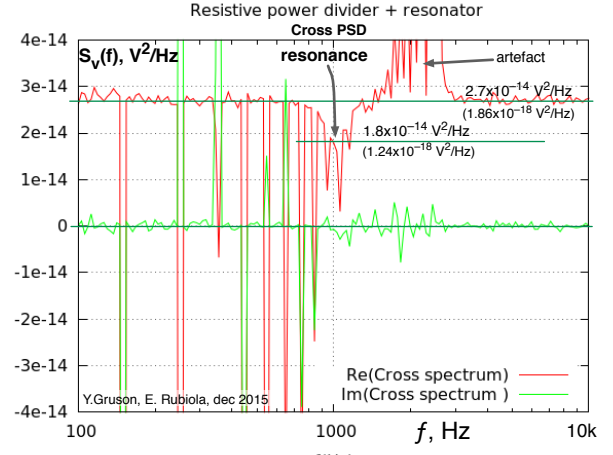


Fig. 5. Cross spectrum measured with the configuration of Fig. 3 B.

At the resonance, Eq. (21) predicts that  $S_{yx} = kT_{ph}R_0$  when the whole system is at the physical temperature  $T_{ph}$ . The value of  $1.25 \times 10^{-18}$ , seen on Fig. 5, is in a close agreement to Eq. (21) with  $T_{ph} = 300$  K and  $R_0 = 300$   $\Omega$ .

Off resonance,  $e_c$  turns into open circuit, and the system changes configuration. From Fig. 2 B, we get

$$S_{yx} = k \left[ \frac{15}{8} T_R^* - \frac{3}{8} T_S \right] R_o$$

assuming that back-scatter temperature of the two receivers is the same and equal to  $T_R^*$ , and that the power splitter is at the temperature  $T_S$ . When the whole system is at the physical temperature  $T_{ph}$ , it holds that

$$S_{yx} = \frac{3}{2} k T_{ph} R_0$$

The value observed on Fig. 5,  $S_{yx} = 1.86 \times 10^{-18}$  V<sup>2</sup>/Hz is in a close agreement to the above formula, again evaluated with  $T_{ph} = 300$  K and  $R_0 = 300$   $\Omega$ . Notice that  $\Im\{S_{yx}\}$  is close to zero at all frequencies, as expected. And of course  $\Re\{S_{yx}\}$  is close to zero at all frequencies.

## VI. CONCLUSION

The internal termination of the input power splitter introduces a systematic error  $\Delta S_\phi$  given by Eq. (18) for the loss-free directional coupler terminated at one end, and by Eq. (25) for the Y resistive splitter.

In most practical cases it holds that  $T_C \gg T_{ph}$ , thus the result is correct for any practical purpose. However, in the case of the low-noise oscillators using the filter, the result can be grossly underestimated because  $T_C$  is just above  $T_{ph}$ .

## ACKNOWLEDGEMENT

This work is partially funded by the ANR ‘‘Programme d’Investissement d’Avenir’’ (PIA) under the Oscillator-IMP project and First-TF network, and by grants from the R gion Franche Comt  intended to support the PIA. We are grateful to Rodolphe Boudot (FEMTO-ST Institute) for the mumetal shields and support, and to Philippe Abb  (FEMTO-ST Institute) for his tough and smart work setting up the shielded chamber and the environment stabilization.

## REFERENCES

- [1] R. Hanbury Brown, R. C. Jennison, and M. K. Das Gupta, "Apparent angular sizes of discrete radio sources," *Nature*, vol. 170, no. 4338, pp. 1061–1063, Dec. 20, 1952.
- [2] R. F. C. Vessot, R. F. Mueller, and J. Vanier, "A cross-correlation technique for measuring the short-term properties of stable oscillators," in *Proc. IEEE-NASA Symposium on Short Term Frequency Stability*, Greenbelt, MD, USA, Nov. 23–24 1964, pp. 111–118.
- [3] F. L. Walls, S. R. Stain, J. E. Gray, and D. J. Glaze, "Design considerations in state-of-the-art signal processing and phase noise measurement systems," in *Proc. Freq. Control Symp.*, Atlantic City, NJ, USA, Jun. 2–4 1976, pp. 269–274.
- [4] W. F. Walls, "Cross-correlation phase noise measurements," in *Proc. Freq. Control Symp.* Hershey, PA: IEEE, New York, 1992, May 27–29 1992, pp. 257–261.
- [5] E. Rubiola and V. Giordano, "Correlation-based phase noise measurements," *Rev. Sci. Instrum.*, vol. 71, no. 8, pp. 3085–3091, Aug. 2000.
- [6] —, "Advanced interferometric phase and amplitude noise measurements," *Rev. Sci. Instrum.*, vol. 73, no. 6, pp. 2445–2457, Jun. 2002.
- [7] C. W. Nelson, A. Hati, and D. A. Howe, "A collapse of the cross-spectral function in phase noise metrology," *Rev. Sci. Instrum.*, vol. 85, no. 3, pp. 024 705 1–7, Mar. 2014.
- [8] "European workshop on cross-spectrum phase noise measurements," LNE Central Site, Paris, France, Dec. 18, 2014.
- [9] "Cross spectrum  $\mathcal{L}(f)$  workshop," Denver, CO, USA, Apr. 15, 2015.
- [10] C. M. Allred, "A precision noise spectral density comparator," *J. Res. NBS*, vol. 66C, pp. 323–330, Oct.–Dec. 1962.
- [11] D. R. White, R. Galleano, A. Actis, H. Brixy, M. De Groot, J. Dubbel-dam, A. L. Reesink, F. Edler, H. Sakurai, R. L. Shepard, and G. J. C., "The status of Johnson noise thermometry," *Metrologia*, vol. 33, pp. 325–335, 1996.
- [12] A. Hati, C. W. Nelson, and D. A. Howe, "Cross-spectrum measurement of thermal-noise limited oscillators," *Rev. Sci. Instrum.*, vol. 87, pp. 2596–2598, Nov. 2012.
- [13] *Keysight E5500 Series, Phase Noise Measurement Solutions*, Keysight Technologies, Inc., Paloalto, CA, 2004, document 5989-0851EN, available online on the web site <http://www.keysight.com>.
- [14] U. L. Rohde, "Crystal oscillator provides low noise," *Electronic Design*, no. 21, pp. 11–14, Oct. 11 1975.
- [15] —, *Microwave and Wireless Synthesizers*. New York: John Wiley & Sons, 1997.